The Journal of Experimental Biology 205, 959–967 (2002)
Printed in Great Britain © The Company of Biologists Limited
JEB3897



# A model of scale effects in mammalian quadrupedal running

Hugh M. Herr[1], Gregory T. Huang[1,*] and Thomas A. McMahon[2,†]

[1]*Harvard/MIT Division of Health Sciences and Technology, Physical Medicine and Rehabilitation, Harvard Medical School, Artificial Intelligence Laboratory, MIT, 200 Technology Square, Room 820, Cambridge, MA 02139, USA* and [2]*Division of Engineering and Applied Science, Harvard University, Cambridge, MA 02138, USA*

*Author for correspondence (e-mail: huang@ai.mit.edu)
†Deceased

*Accepted 23 January 2002*

## Summary

**Although the effects of body size on mammalian locomotion are well documented, the underlying mechanisms are not fully understood. Here, we present a computational model of the mechanics, control and energetics that unifies some well-known scale effects in running quadrupeds. The model consists of dynamic, physics-based simulations of six running mammals ranging in size from a chipmunk to a horse (0.115–676 kg). The 'virtual animals' are made up of rigid segments (head, trunk and four legs) linked by joints and are similar in morphology to particular species. In the model, each stance limb acts as a spring operating within a narrow range of stiffness, forward motion is powered and controlled by active hip and shoulder torques, and metabolic cost is predicted from the time course of supporting body weight. Model parameters that are important for stability (joint stiffnesses, limb-retraction times and target positions and velocities of the limbs) are selected such that (i) running kinematics (aerial height, forward speed and body pitch) is smooth and periodic and (ii) overall leg stiffness is in agreement with published data. Both trotting and galloping gaits are modeled, and comparisons across size are made at speeds that are physiologically similar among species. Model predictions are in agreement with data on vertical stiffness, limb angles, metabolic cost of transport, stride frequency, peak force and duty factor. This work supports the idea that a single, integrative model can predict important features of running across size by employing simple strategies to control overall leg stiffness. More broadly, the model provides a quantitative framework for testing hypotheses that relate limb control, stability and metabolic cost.**

Key words: biomechanics, locomotion, running, mammal, quadruped, body size, leg stiffness, metabolic cost of transport, computational model, limb control.

## Introduction

Body size has a profound impact on many aspects of animal physiology and ecology, including locomotion (Schmidt-Nielsen, 1984; Calder, 1996). On a mass-specific basis, small animals use stiffer legs (Farley et al., 1993) and more metabolic energy (Taylor et al., 1970) than large animals to run a given distance. At their lowest galloping speeds, small mammals sweep through larger hindlimb excursion angles (McMahon, 1975) and use greater stride frequencies (Heglund et al., 1974) than large mammals. These data can be used to test models that relate body design to performance on the basis of assumptions of muscle mechanics and anatomical scaling. For example, a model of geometric similarity, in which all linear dimensions of the body change by the same scale factor, makes predictions of gait performance *versus* size (Hill, 1950). Although this structural assumption has support over a wide range of species (Alexander et al., 1979; Biewener, 1983), some of the gait predictions are inconsistent with the data (McMahon, 1975). In contrast, the model of elastic similarity, in which lengths and diameters of the body scale differently, predicts gait data more successfully (McMahon, 1973, 1975), but its structural assumptions hold only among closely related species (Alexander et al., 1979; Alexander, 1988).

To capture the diversity of animal design and locomotory performance, more detailed models of morphology, musculoskeletal mechanisms and motor control are needed (Full and Koditschek, 1999; Kubow and Full, 1999). Here, we develop a model of running that is based on the body structure and stride-to-stride dynamics of a variety of quadruped species. This work builds upon recent computer simulations of a running horse (Herr and McMahon, 2000, 2001) by extending the theory to animals of different size.

The broad aim of this work is to explain how the extensive data on locomotory scale effects are related. It is not fully understood, for example, how the size-dependence of leg stiffness and limb excursion angle in trotting and galloping quadrupeds may be related to the size-dependence of the metabolic cost of transport. Here, we hypothesize that a single, integrative model of mechanics, control and energetics can

predict how important features of running change with size in mammalian quadrupeds. To test the hypothesis, we conduct computational experiments on six morphologically realistic animal models ('virtual animals') ranging in size from a chipmunk (0.115 kg) to a horse (676 kg). Each virtual animal trots and gallops in numerical simulations using the following set of biologically plausible strategies, to be justified below: (i) each stance limb acts as a linear spring of constant stiffness (Cavagna et al., 1988; Blickhan, 1989; McMahon and Cheng, 1990); (ii) forward motion is powered and controlled by active hip and shoulder torques; and (iii) metabolic cost is predicted from the time course of supporting body weight (Kram and Taylor, 1990). With overall leg stiffness constrained by published experimental data (Farley et al., 1993), we select model parameter values such that the virtual animals remain upright and the running kinematics is smooth and periodic. Finally, we test the model for internal consistency by comparing the simulation results with available experimental data. We would reject the model's set of assumptions if we were to find discrepancies between predictions and data (e.g. in metabolic cost).

To summarize, we ask whether there exists a set of biologically plausible locomotory principles that, when specified in the formulation of our model, unifies well-known features of quadrupedal trotting and galloping across body size. It is our belief that answering this question will be a step towards identifying mechanisms of gait performance in a wide variety of terrestrial mammals and, ultimately, a more unified theory of locomotory mechanics, control and energetics.

## Materials and methods

### *Model structure*

Six virtual animals were constructed to simulate the stride-to-stride running dynamics of two horses (676 kg and 134 kg), a goat (25.2 kg), two dogs (23.9 kg and 5.09 kg) and a chipmunk (0.115 kg) (Fig. 1). Each virtual animal consisted of 11 rigid body segments connected by joints: three segments for the head and trunk, and two segments for each leg. The legs were connected to the trunk at shoulder and hip pin joints, enabling each limb to rotate in the sagittal plane. As back and neck flexion is observed in running quadrupeds (Muybridge, 1957) and since these motions affect the mechanics of running (Alexander, 1985, 1988), back and neck joints were included in the model. The head was free to rotate about a pin joint located at the base of the neck, and a back pin joint was located half-way between the tail base and the caudal aspect of the rib cage, where spine flexion is maximal (Alexander, 1985).

Similar to the horse model of Herr and McMahon (2000, 2001), each limb was formed with an upper and a lower segment connected by a prismatic (telescoping) joint such that the limb could change length. The simplifying assumption of prismatic joints for the elbows and knees was justified because the quadruped limbs were lightweight (limb mass <7 % of total body mass) (Fedak et al., 1982), so that hip and shoulder torques to accelerate each limb were small compared with those required to sustain forward running. Consequently, errors

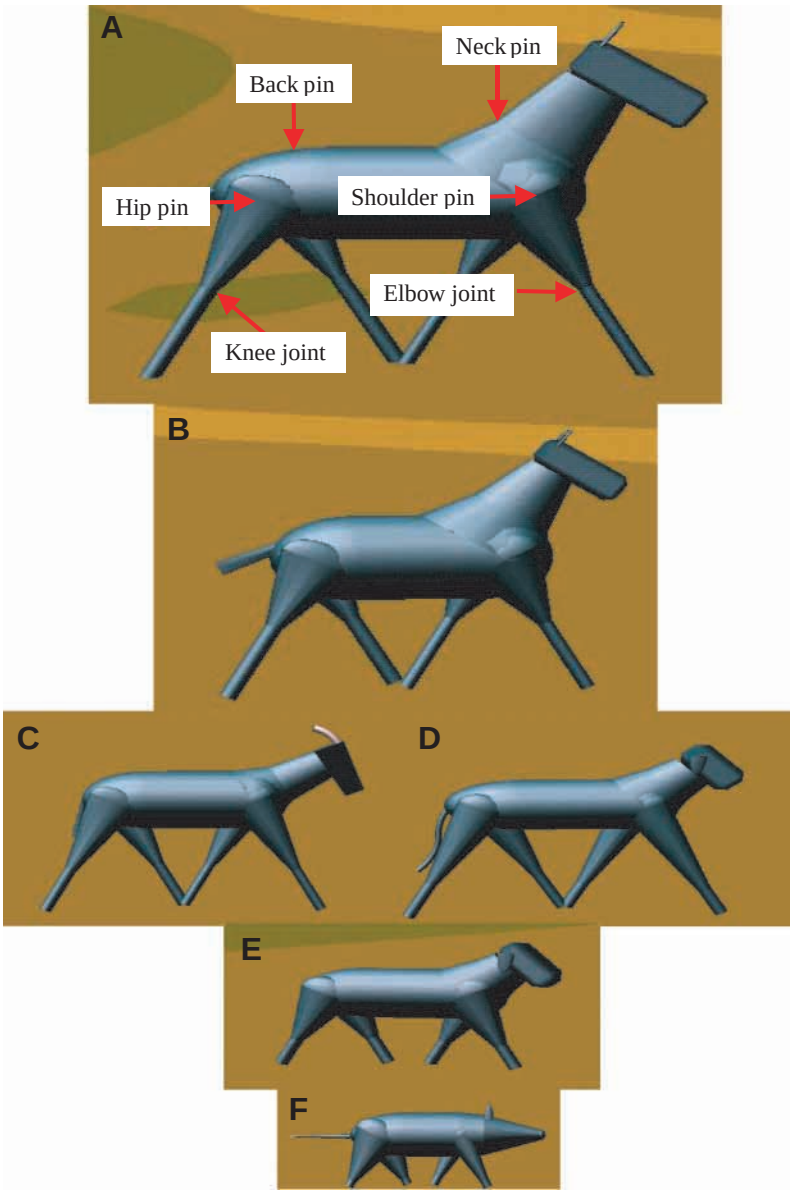


Fig. 1. Model structure: (A) large horse, (B) small horse, (C) goat, (D) large dog, (E) small dog and (F) chipmunk. Joint locations, segment dimensions and mass distributions are from photographic, video and anatomical data (Muybridge, 1957; Taylor et al., 1974; Fedak et al., 1982; Alexander, 1985; Farley et al., 1993). All segments are represented as rigid bodies. Pin (rotary) joints are included on the back and neck. Each leg rotates about a pin joint at the shoulder or hip and changes length through a prismatic (telescoping) joint at the elbow or knee. Active hip and shoulder torques control the forward motion from stride to stride. Motions are restricted to the sagittal plane.

in limb moments of inertia from the prismatic assumption led to negligible errors in total torque output.

For this study, we did not use an average quadrupedal form; rather, the virtual animals were given mass distributions and shapes similar to those of particular species. Joint locations and segment lengths were measured from the animal photographs of Muybridge (1957) or, in the case of the chipmunk model, from video camera images (200 frames $s^{-1}$) of a running chipmunk. The back flexion point, hip-to-shoulder distance, neck and head lengths, shoulder-to-elbow distance and hip-to-knee distance were all measured from photographic or video images and normalized to leg length. The back flexion point was measured by estimating the midway point between the tail base and the caudal aspect of the rib cage. The shoulder-to-hip distance was measured from a point midway between the greater tubercle and the dorsal aspect of the scapula and the greater trochanter of the femur. The distance from the elbow to the shoulder point and the distance from the knee to the hip point were also measured from the animal images.

These dimensionless sagittal-plane lengths were then multiplied by the animal's leg length. Leg lengths were taken from the literature (Fedak et al., 1982; Farley et al., 1993), except for the large horse's leg length, which was measured directly on a horse specifically for the study. Each leg length was computed using the protocol of Farley et al. (1993) by taking the average of the forelimb and hindlimb lengths at first contact in trotting. The forelimb length was taken as the distance from the foot to a point midway between the greater tubercle and the dorsal aspect of the scapula and the hindlimb length as the distance from the foot to the greater trochanter of the femur. Mass was distributed throughout each virtual animal in a realistic manner using data from the literature (Taylor et al., 1974; Fedak et al., 1982). The lateral thicknesses of the trunk, neck and limbs were computed using the mass of each segment, the sagittal-plane lengths and the volume formula for each segment shape.

### *Biological assumptions of the model*

For the virtual animals to be viewed as plausible biological representations, three main assumptions were made irrespective of size and gait. First, each limb behaved as a linear spring of constant stiffness throughout each ground-contact phase in running. During stance, a limb changed length through a passive telescoping joint whose stiffness was linear and invariant with time. The support for this assumption includes linear measurements of force *versus* displacement in mammalian limbs and agreement of bouncing spring-mass models with gait data (Cavagna et al., 1988; Blickhan, 1989; McMahon and Cheng, 1990; Blickhan and Full, 1993). Second, forward motion was controlled by active torques about the proximal leg joints (hips and shoulders); these torques were the only energy input to the model during stance. This assumption was made to achieve a simple control scheme that was biologically realistic. Anatomical descriptions of limb musculature and measurements of ground-reaction forces from trotting dogs are consistent with this assumption (Gray, 1968; Lee et al., 1999). Third, metabolic cost of running was predicted from the cost of supporting body weight and the time course of generating that force. This last assumption was based on evidence that, during running, the metabolic rate is inversely proportional to the time per stride that a given foot contacts the ground (Kram and Taylor, 1990). It allowed metabolic costs to be calculated from the kinematics of the virtual animal simulations. There are other approaches for estimating the metabolic cost of locomotion on the basis of external mechanical work (Taylor et al., 1982; Full, 1989; Donelan et al., 2002); we used the rule of Kram and Taylor (1990) because of its simplicity and because it was tested on species similar to those in this study.

### *Gaits*

Two distinct quadrupedal gaits were modeled: trotting and galloping. During trotting, diagonal pairs of limbs moved approximately in concert, with one pair on the ground at a time. During galloping, which was used at higher speeds, the four limbs touched the ground sequentially during each contact period. The present model did not attempt to explain why a particular gait was used at a given speed. Rather, for each speed, experimental observations were used to select the relevant gait. Interspecies comparisons were made at physiologically equivalent speeds (Heglund et al., 1974) (Table 1). For trotting, model predictions and measurements were compared near the midpoint of each animal's natural range of trotting speeds, with similar Froude numbers and duty factors occurring among species (Alexander, 1988; Heglund and Taylor, 1988; Farley et al., 1993). The Froude number was defined as $u/(\boldsymbol{g}L_0)^{1/2}$, where $u$ is forward speed (averaged over a stride), $\boldsymbol{g}$ is gravitational acceleration and $L_0$ is leg length. Duty factor was defined as the percentage of a stride period during which a foot was on the ground. For galloping, comparisons were made at each animal's lowest galloping speed, i.e. its trot–gallop transition speed (Heglund et al., 1974; Heglund and Taylor, 1988).

### *Model control implementation*

The dynamics of trotting and galloping were simulated by programming motor control into the model structures, subject to the laws of Newtonian mechanics. A commercially available software package (SD/Fast, Symbolic Dynamics Inc.) was employed to generate and integrate the non-linear equations of motion using a fourth-order Runge–Kutta method (0.4 ms time step). Local software enabled communication between the control algorithms and SD/Fast to determine the forces and torques commanded to the joints. All running simulations were two-dimensional, operating within the sagittal plane. Yaw and roll degrees of freedom were neglected.

### *Parameter definitions*

For the virtual animals to trot and gallop in numerical simulation, mechanical and kinematic control parameters needed to be defined (see Table 1 for key parameters). The mechanical parameters were the stiffnesses of the limbs (at the

Table 1. *Key parameters of the model*

| | Mass (kg) | Leg length (m) | Forelimb stiffness ($kN\,m^{-1}$) | Hindlimb stiffness ($kN\,m^{-1}$) | Trotting Speed ($m\,s^{-1}$) | Trotting Forelimb target speed ($rad\,m\,s^{-1}$) | Trotting Hindlimb target speed ($rad\,m\,s^{-1}$) | Trotting Neck stiffness ($kN\,m\,rad^{-1}$) | Trotting Back stiffness ($kN\,m\,rad^{-1}$) | Galloping Speed ($m\,s^{-1}$) | Galloping Forelimb target speed ($rad\,m\,s^{-1}$) | Galloping Hindlimb target speed ($rad\,m\,s^{-1}$) | Galloping Neck stiffness ($kN\,m\,rad^{-1}$) | Galloping Back stiffness ($kN\,m\,rad^{-1}$) |
|---|---|---|---|---|---|---|---|---|---|---|---|---|---|---|
| Chipmunk | 0.115 | 0.048 | 0.097 | 0.077 | 1.2 | 0.9 | 1.1 | 0.001 | 0.002 | 1.8 | 1.5 | 1.9 | 0.001 | 0.002 |
| Dog 1 | 5.09 | 0.20 | 1.9 | 1.2 | 1.9 | 1.5 | 1.8 | 0.03 | 0.013 | 2.8 | 2.5 | 3.1 | 0.005 | 0.025 |
| Dog 2 | 23.9 | 0.50 | 2.9 | 1.9 | 2.9 | 2.4 | 3.2 | 0.15 | 0.01 | 4.0 | 3.5 | 4.5 | 0.20 | 0.10 |
| Goat | 25.2 | 0.48 | 4.9 | 2.7 | 2.8 | 2.3 | 3.1 | 0.19 | 0.015 | 3.2 | 2.8 | 3.6 | 0.20 | 0.10 |
| Horse 1 | 134 | 0.75 | 18 | 9.1 | 2.7 | 2.3 | 3.0 | 1.0 | 1.7 | 5.2 | 4.3 | 6.1 | 1.0 | 1.7 |
| Horse 2 | 676 | 1.5 | 37 | 22 | 3.9 | 3.2 | 4.6 | 11.0 | 8.0 | 5.8 | 4.8 | 6.7 | 9.0 | 17 |

Masses and leg lengths are based on published data (Fedak et al., 1982; Farley et al., 1993).
Comparisons among species are made at physiologically similar running speeds (Alexander, 1988; Heglund and Taylor, 1988).
The basic control methods are invariant with size. Mechanical and control parameters are constrained to satisfy smooth, periodic running dynamics and biologically realistic leg stiffness. The parameters listed determine the dynamics of each ground-contact phase and are critical to the constraints.
The values of limb-joint stiffnesses are used for both trotting and galloping, whereas back and neck stiffnesses are gait-specific.
Limb target speeds are the desired tangential velocities of the feet (relative to the hip and shoulder) during stance.

telescoping joints), back and neck during ground contact. These passive properties, which were fixed for the duration of ground contact (the first assumption of the model), helped to determine the behavior of each virtual animal as it rebounded from the ground during trotting and galloping. The kinematic control parameters were target limb-retraction speeds and gains, aerial position and velocity gains, target joint positions and limb-retraction times. To control forward running speed in trotting or galloping, torques were applied about the hip and shoulder (the second assumption of the model) such that the tangential velocity component of each foot, measured relative to each foot's proximal hip or shoulder joint, was sustained. The target limb-retraction speeds were the desired tangential velocities of the feet relative to the hip and shoulder during ground contact. There were two target speeds, one corresponding to the forelimbs and a second corresponding to the hindlimbs. Foot velocity was computed by multiplying the virtual animal's leg length by the angular velocity of the hip or shoulder joint measured relative to the trunk. The applied torque was set proportional to the difference between a measured tangential velocity component and a target limb-retraction speed. To control forward speed in trotting and galloping simulations, this proportionality constant, or gain, was defined together with two limb-retraction speeds corresponding to the fore- and hindlimbs (Herr and McMahon, 2000, 2001).

During each aerial phase, conventional proportional-plus-derivative (PD) controllers (Nise, 1995) (pp. 460–469) were used to position the hip, shoulder, back and neck joints to desired angular positions relative to the model trunk in preparation for landing. PD controllers were also used to shorten the limbs for foot clearance and then to lengthen the limbs for landing. Here, the force or torque applied to a joint was proportional to errors in position and velocity.

After achieving a desired position, each limb retracted just before striking the ground. Retraction times were set by an internal clock (analogous to a neural pattern generator) that determined how the limbs were phase-locked in a trot or gallop. Throughout this paper, limb retraction is defined as a backward displacement of the foot by means of rotating a limb about the hip or shoulder joint within the sagittal plane (Gray, 1968). In trotting simulations, a diagonal limb pair began to retract towards the ground after a fixed time interval from the beginning of the aerial phase. In galloping simulations, the retractions of the first hindlimb and the first forelimb to strike the ground were separated by fixed time intervals; the second hindlimb began to retract when the first hindlimb became perpendicular with the trunk, and similarly, the second forelimb began to retract when the first forelimb became perpendicular with the trunk.

### *Setting model parameters*

The first constraint on the model parameters was that simulations were required to be smooth and periodic. For each gait (trotting and galloping) and for each virtual animal, we adjusted the model parameters to achieve this condition. Periodicity was defined as no significant change ($P<0.05$) in the

animal's maximum aerial height, forward speed and body pitch over 20 running cycles. Running simulations were started with the animal off the ground. Initial conditions were defined for the position and velocity of the center of mass and the individual body segments. When periodicity was satisfied, we found that the simulation dynamics was insensitive to the initial conditions. When periodicity was not satisfied, however, simulation dynamics was found to be strongly dependent on the initial conditions and, typically, a simulation run would become unstable within only a few strides. For the small horse simulations, we demonstrated the model's capacity to recover from an environmental disturbance: a sudden 20 % reduction in ground stiffness (Herr and McMahon, 2000, 2001). These numerical experiments suggested that periodicity may be related to dynamic stability, but in no way served as proof of stability.

Simulation experiments showed that the model's cyclic behavior was sensitive to variations (among simulation runs) in fore- and hindlimb stiffnesses during stance, target limb-retraction speeds, target limb angle and limb-retraction times. To set these parameters, genetic algorithms were employed to search the parameter space for smooth and periodic behavior. Specifically, we performed a genetic-algorithm search (Goldberg, 1989) to find these control values that minimized the variance in step-to-step maximum aerial height, forward speed and body pitch. The resulting ranges of parameter values demonstrated the mechanical correlates of the periodicity constraint. Most notably, we found that stance-limb stiffnesses must exceed certain minimum values to keep the body upright from stride to stride. Below this stiffness threshold, each virtual animal could be stabilized, but only with active limbs, i.e. when non-conservative forces were applied along the axis of the limb (see Herr and McMahon, 2000).

The second constraint on model parameters was that the overall leg stiffness ($k_{leg}$) for each animal should match published experimental data. It is important to point out that $k_{leg}$ represents the stiffness of the entire musculoskeletal system during stance (McMahon and Cheng, 1990; Farley et al., 1993). The method for computing $k_{leg}$ is reviewed in the next section. From the sets of parameter values that led to smooth and periodic trotting, we chose the particular set of values that led to the closest agreement between the computed $k_{leg}$ and experimental $k_{leg}$ values from the literature. That is, after stabilizing the model, we tuned the fore- and hindlimb stiffnesses, target limb-retraction speeds, target limb angle and retraction times to match the $k_{leg}$ data. The data are well-fitted by the power law $k_{leg}=0.715M^{0.67}$, where $M$ is the body mass of the animal in kg, and the units of $k_{leg}$ are kN m$^{-1}$ (Farley et al., 1993). The same fore- and hindlimb stiffness values were used in galloping and in trotting simulations.

For trotting and galloping simulations, we also adjusted model parameters that had little effect on periodicity or overall leg stiffness, such as neck and back stiffness during stance and aerial-phase PD gains. Neck and back stiffnesses were selected to minimize the number of oscillations in the trunk per stride, and aerial PD gains (position and velocity) were set to position the joints such that each joint moved to its target position without overshoot. For all PD controllers, target velocities were set to zero.

The ground was modeled with linear springs and dampers in the vertical and horizontal directions to model the viscoelastic properties of a natural running surface. Ground stiffness was first set so that the limbs penetrated the ground by a small amount when running (0.3 cm for the small horse model). Increasing damping from zero then minimized oscillations between the ground and foot.

### *Model outputs*

The model's outputs were computed from the dynamics of each set of animal simulations as follows. For trotting animals, leg stiffness was defined as $k_{leg}=F/\Delta l$, where $F$ is the peak vertical ground-reaction force and $\Delta l$ is the compression of a virtual leg spring, based on a spring-mass representation of the center of mass as it rebounded from the ground (McMahon and Cheng, 1990; Farley et al., 1993). The spring compression was given by $\Delta l=\Delta y+L_0(1-\cos\theta)$, where $\Delta y$ is the vertical displacement of the center of mass during stance, $\theta=\sin^{-1}(ut_c/2L_0)$ is the virtual-leg angle from vertical at touchdown (or half the angle swept by the leg during stance), $t_c$ is the foot-contact time per stride and $L_0$ is leg length. Vertical stiffness was defined as $k_{vert}=F/\Delta y$ and described the center-of-mass mechanics of the stance phase in the vertical direction.

In the model, these properties of overall stiffness depended on the joint stiffnesses, target limb positions and target retraction speeds. (The stiffnesses $k_{leg}$ and $k_{vert}$ are defined for symmetrical gaits such as trotting, hopping and bipedal running, but they do not describe the mechanics of galloping.) Cost of transport (COT) was defined as the metabolic energy required to move a unit mass over a unit distance (Taylor et al., 1970; Schmidt-Nielsen, 1984). In the model, COT was computed from the kinematics of the animal simulations (the third assumption of the model) based on the empirical rule $\mathrm{COT}=C_0/ut_c$, where $u$ is forward speed and $C_0$ ($C_0=1.8\,\mathrm{J\,kg^{-1}}$) was a size- and speed-independent cost coefficient (Kram and Taylor, 1990). In this work, the empirical rule of Kram and Taylor served as a bridge between model mechanics and energetics.

For galloping, we calculated stride frequency, hindlimb excursion angle, forelimb duty factor, peak vertical ground-reaction force and the cost of transport. These output variables depended primarily on limb stiffness (fore- and hindlimb) and the parameter values (target limb positions, target limb speeds, retraction times) resulting from the genetic-algorithm search for smooth and periodic solutions. We set the cost coefficient $C_0$ to 1.8 J kg$^{-1}$ (as in trotting), the forward speed $u$ to the minimum galloping speed (trot–gallop transition speed; Table 1) and $t_c$ to the mean contact time predicted from the galloping simulations.

## Results

### *Mechanical and kinematic control parameters*

The model's parameters provided a theoretical glimpse into the workings of our virtual animals. After enforcing the

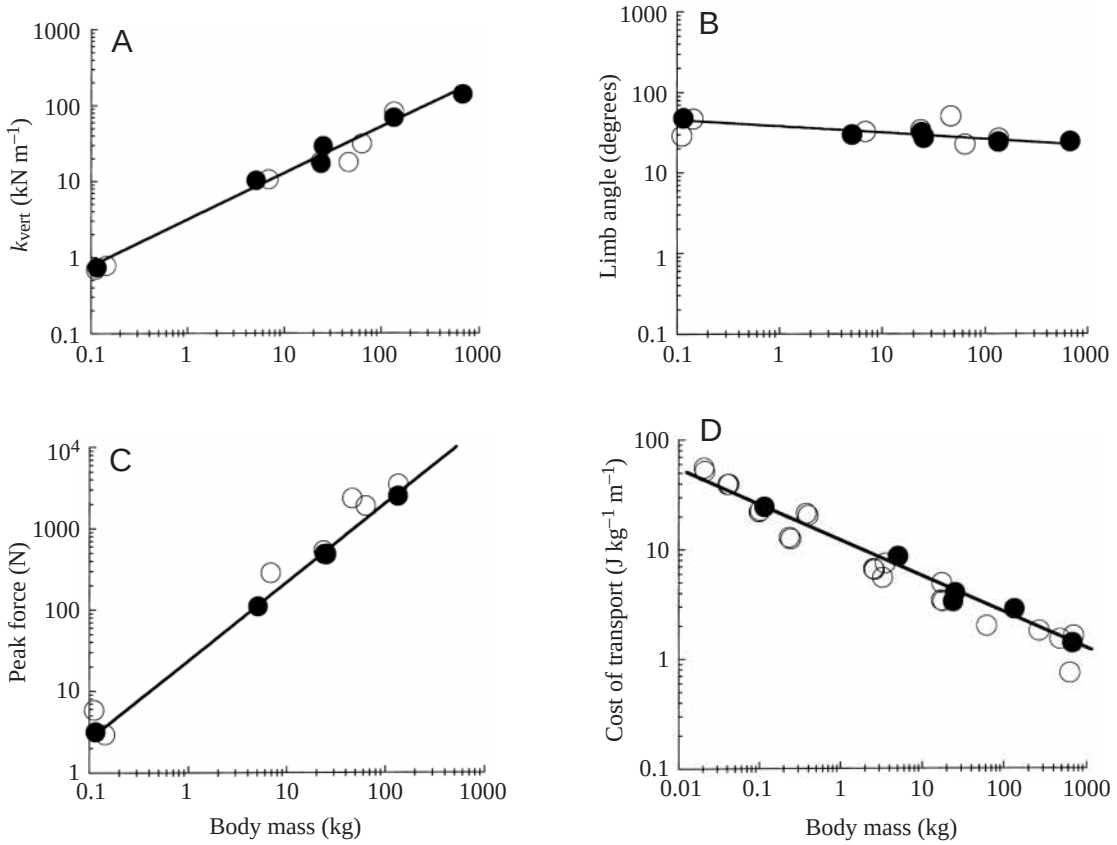


Fig. 2. Mechanical and energetic properties of trotting animals at the preferred trotting speed plotted *versus* body mass on logarithmic scales. Open circles are mean experimental values, and filled circles are model predictions. Least-squares regression lines are fitted to the model results (see text for equations). (A) Vertical stiffness, $k_{vert}$. (B) Limb angle from the vertical at touchdown. (C) Peak vertical ground-reaction force. (D) Metabolic cost of transport. Animal data are adapted with permission from Farley et al. (1993) (A–C) and from Taylor et al. (1970, 1982) (D). Data include measurements from horses, goats, dogs and rats.

constraint of stride-to-stride smoothness and periodicity, we discovered that, in general, forelimb stiffnesses needed to be greater than hindlimb stiffnesses by an average of 64 % (see Table 1). This is perhaps accounted for by the fact that the head and neck masses were a significant fraction of total body mass (13 % on average), requiring that the forelimbs be stiffer than the hindlimbs to keep the animal upright from stride to stride. We also found that the hindlimb target speeds needed to be greater than the forelimb target speeds by an average of 31 % for trotting and 32 % for galloping. With this model control, smooth and periodic solutions were found without the use of pitch orientation as a sensory input; the virtual animals ran without sensory knowledge of absolute body orientation.

### *Trotting performance*

In this section, we compare the model predictions for trotting with experimental data. The model's leg stiffness ($k_{leg}$) was constrained to match published data (Farley et al., 1993), as described in Materials and methods. This constraint, together with the requirement for smooth and periodic trotting solutions, led to predictions of vertical stiffness, limb angle, peak force and the cost of transport *versus* body mass (Fig. 2). Least-squares regression lines were fitted to the simulation results (filled circles, $N$=6) and compared with experimental data (open circles). The linear regressions (with units of the variables as plotted) are: vertical stiffness ($k_{vert}=3.2M^{0.61}$, $r^2=0.98$); limb angle from the vertical at touchdown ($\theta=38M^{-0.081}$, $r^2=0.91$); peak vertical ground-reaction force ($F=24M^{0.96}$, $r^2=0.99$); and cost of transport ($COT=12M^{-0.33}$, $r^2=0.99$). Least-squares regression lines fitted to the experimental data of Farley et al. (1993) and Taylor et al. (1970, 1982) are $k_{vert}=2.64M^{0.61\pm0.10}$, $\theta=34.35M^{-0.034\pm0.092}$, $F=30.1M^{0.97\pm0.14}$; and $COT=10M^{-0.36\pm0.09}$, where the uncertainties are standard errors on the slope. We conclude that the model predictions for trotting are in quantitative agreement with published experimental data on mechanical and energetic properties *versus* size.

### *Galloping performance*

In this section, we compare the model predictions for galloping with experimental data. With the same values for fore- and hindlimb stiffness as used in the trotting simulations, the constraint of stride-to-stride smoothness and periodicity led to predictions of stride frequency, limb excursion angle, duty factor and peak vertical ground-reaction force (Fig. 3). Least-squares regression lines were fitted to the simulation results (filled circles, $N$=6) and compared with experimental data

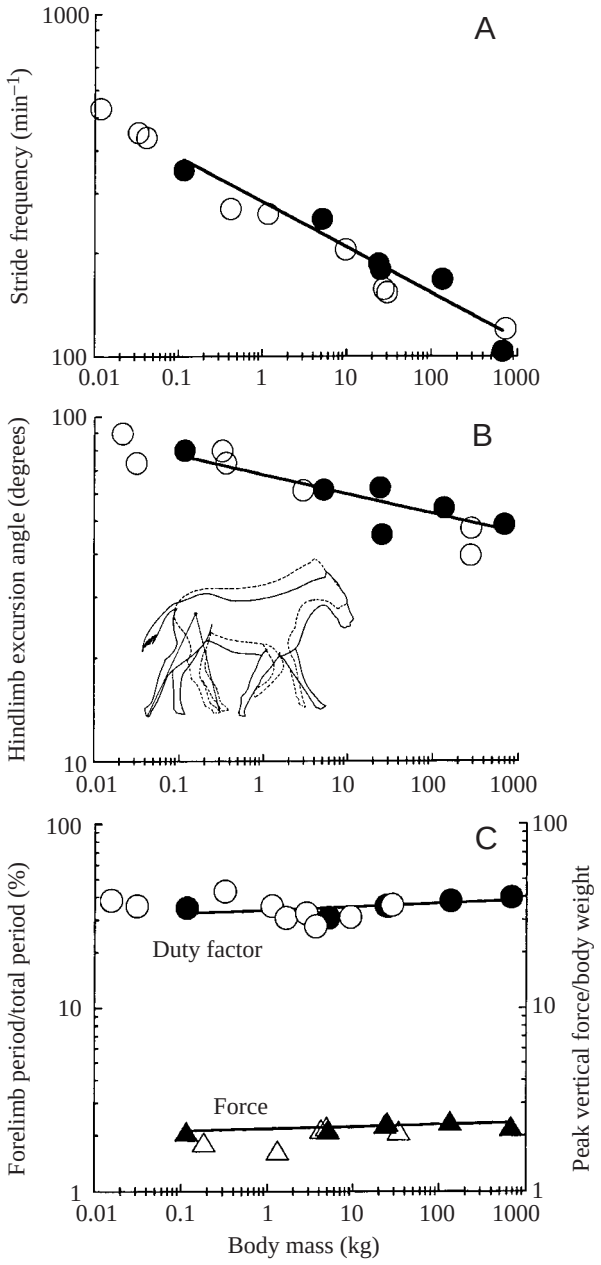


Fig. 3. Mechanical properties of galloping animals at the trot–gallop transition speed plotted *versus* body mass on logarithmic scales. Open circles are experimental values, and filled circles are model predictions. Least-squares regression lines are fitted to the model results (see text for equations). (A) Stride frequency. (B) Hindlimb excursion angle, the maximum angle swept by a line drawn from the head of the femur to the toe. (C) Forelimb duty factor, the percentage of a stride period in which a forelimb contacts the ground, and peak vertical force per body weight. Animal data are adapted with permission from (A) Heglund et al. (1974), (B) McMahon (1975) and (C) McMahon (1977). Data were taken from horses, dogs, squirrels, rats and mice.

(open circles). The linear regressions are: stride frequency ($f_S$), in cycles per minute ($f_S=282M^{-0.13}$, $r^2=0.96$); hindlimb excursion angle ($\alpha$) ($\alpha=68M^{-0.06}$, $r^2=0.77$); forelimb duty factor (DF) ($DF=34M^{0.018}$, $r^2=0.45$) and peak vertical force ($F$) per body weight ($F/M\boldsymbol{g}=2.2M^{0.011}$, $r^2=0.43$). Least-squares regression lines fitted to the experimental data are $f_S=269M^{-0.14\pm0.01}$, $\alpha=66M^{-0.07\pm0.01}$, $DF=34M^{-0.03\pm0.02}$ and $F/(M\boldsymbol{g})=2M^{0.04\pm0.03}$, where the uncertainties are standard errors on the slope. We conclude that the model predictions of galloping mechanics *versus* size at the minimum galloping speed are generally in quantitative agreement with published experimental data.

The energetic predictions for galloping are also in agreement with experimental animal data. A least-squares regression line for the model's cost-of-transport (COT) values *versus* mass plotted on double logarithmic coordinates gives $COT=14M^{-0.36}$ ($r^2=0.95$, $N=6$). This model prediction is in agreement with the cost of transport allometric equation $COT=14.6M^{-0.37\pm0.1}$, adapted with permission from Heglund and Taylor (1988). The uncertainties are 95% confidence limits for the slope.

## Discussion

### *Overview*

In this paper, we hypothesized that a single, integrative model of mechanics, control and energetics could predict how some well-known features of running would change with size in mammalian quadrupeds. To test the hypothesis, we applied biologically plausible strategies of animal movement to six morphologically realistic virtual animals spanning nearly three orders of magnitude in body size. We compared the model dynamics in trotting and galloping simulations with experimental data to test the model assumptions for internal consistency. Parameters were not tuned to match the data set used to test the model. Rather, the model parameters were selected for smooth and periodic running solutions, and the overall leg stiffness of each virtual animal was constrained by published data (Farley et al., 1993). We found model predictions to be in agreement with the data not only for mechanical variables but also for the rate of energy metabolism, providing support for our hypothesis. Moreover, we demonstrated internal consistency between biological values of leg stiffness, the rule of Kram and Taylor (1990) for metabolic cost of transport and a relatively simple cycle-to-cycle control scheme.

### *Significance of model control*

It is important to point out that the overall behavior of the model was strongly dependent on the methods used for pitch and speed control. In investigations of alternative control schemes, we found strategies that kept the virtual animals upright from stride to stride but with features grossly inconsistent with biological data. For example, when forward speed was sustained by actively extending the contact limbs beyond their equilibrium lengths at the end of stance (by applying non-conservative forces about the knee and elbow), the vertical oscillations of the body increased dramatically and the gait resembled a bound (see Hildebrand, 1976) rather than a trot or gallop, with a vertical stiffness much smaller than those measured in animals (see Fig. 2A).

In developing the model, such alternative strategies were rejected in favor of more biologically plausible control methods (Herr and McMahon, 2000). Given the realistic morphology of the virtual animals, the control features responsible for their realistic dynamics were passive springy legs and active wheel-like limb control. Here, the axial limb response (fore- and hindlimbs) was passive and spring-like throughout stance, while active hip and shoulder torques rotated each stance limb such that the tangential velocity component of each foot was sustained like the rim of a steadily rolling wheel. The model's requirements for sensory information (e.g. joint positions and velocities) and active joint-torque magnitudes (e.g. 120 N m at the hip and shoulder of the small horse) did not exceed the reported capabilities of mammals (Eyzaguirre and Fidone, 1975; Roberts, 1995; Herr and McMahon, 2000, 2001). The model's control thus represents a set of simple, plausible rules by which running quadrupeds might operate.

### *Implications for running mechanics and motor control*

For both trotting and galloping, the constraint of smooth and periodic solutions led to the selection of hindlimb target speeds that were greater than the forward speed of running and of forelimb target speeds that were less than the forward speed (Table 1). This relationship between the target speeds caused the hip generally to apply a thrusting torque (supplying mechanical energy) and the shoulder a braking torque (dissipating energy). When the forelimb speed was greater than the hindlimb speed, the model was unstable. This result suggests that thrusting hip torques and braking shoulder torques may be crucial for dynamic stability. This strategy is qualitatively consistent with ground-force measurements in running dogs (Lee et al., 1999; Herr and McMahon, 2000).

The size-dependencies of stride frequency and excursion angle in galloping (Fig. 3) have previously been explained as mechanical constraints of natural frequencies of vibration and muscle force acting across a joint, respectively (McMahon, 1975). The present model provides an alternative explanation. Our results suggest that biological values of stride frequency and excursion angle may arise from interactions between motor control and stride-to-stride dynamics. We found that the timing of limb movements was crucial to stability and changed with the size of the model, suggesting that neural pattern generators that control limb movements might be tuned for stability as a function of body size. The emergent model behaviors of duty factor and normalized peak force were relatively invariant with size, which is consistent with experimental data (Fig. 3C). The agreement between model predictions and experimental data for both trotting and galloping supports the idea that, in addition to mechanical considerations, stride-to-stride periodicity constrains scale effects in running quadrupeds.

Irrespective of size, animals must sustain their forward speed and remain balanced while running. However, it is not known whether different control strategies are required to stabilize animals of different size or whether species have evolved with altogether different strategies for optimizing running economy and/or speed. In this paper, a single control strategy was used to stabilize six virtual animals spanning nearly three orders of magnitude in body size. This control-independence suggests that scale effects in quadrupedal running are attributable primarily to morphological differences among animals, not to fundamental differences in how they remain balanced from stride to stride. As animals get larger, the basic control scheme required to maintain stability need not change, but the stiffness and timing of limb movements change on the basis of the morphology of the limbs, trunk and head. This result supports the idea that the natural dynamics of the body simplify the control of locomotion (Raibert and Hodgins, 1993; Kubow and Full, 1999).

For each virtual animal, smooth and periodic trotting solutions were found when we increased $k_{leg}$ or stride frequency above the biological range, with the disadvantage of increasing the predicted cost of transport (Herr and McMahon, 2000). However, when we decreased $k_{leg}$ or stride frequency below the biological range, smooth and periodic solutions could not be found. We speculate that the biological range of $k_{leg}$ may represent a minimum-stiffness boundary for stability. At these stiffness values, the predicted cost of transport, which is in agreement with the data (Fig. 2D), may represent the lowest metabolic energy level within the region of stiffness where stability can be achieved with passive, spring-like legs. This explanation of biological stiffness values seems plausible, given the evidence that energy consumption is minimized by gait transitions in humans and horses (Margaria, 1976; Hoyt and Taylor, 1981), and warrants further investigation.

### *Concluding remarks*

Perhaps the simplest summary of our findings is that the present model, constrained by periodicity and stiffness and incorporating empirical energetics, predicted a substantial data set across size on the basis of simple mechanical and control features. Further development of the model may include an investigation of the determinants of leg stiffness, the incorporation of virtual muscle mechanics to derive energetic properties from first principles, the representation of limb postures to test whether postural variations with size (Biewener, 1983, 1989) are constrained by stability and extension to bipedal running. Before this work, it had not been shown that the size-dependent properties of quadrupedal running could be unified within a single theoretical framework. In the study of body size to understand locomotory function, we believe that identifying mechanisms critical to stability and metabolic economy can lead to simple ways to think about how animals operate.

We thank Max Berniker, Andrew Biewener, Reinhard Blickhan, Robert Full, Rodger Kram and Andre Seyfarth for comments on the manuscript. This work was supported in part by the Michael and Helen Shaffer Foundation and by funds from Phil Carvey for rehabilitation research.

## References


**Alexander, R. McN.** (1985). Elastic structures in the back and their role in galloping in some mammals. *J. Zool., Lond.* **207**, 467–482.

**Alexander, R. McN.** (1988). *Elastic Mechanisms in Animal Movement*. Cambridge: Cambridge University Press.

**Alexander, R. McN., Jayes, A. S., Maloiy, G. M. O. and Wathuta, E. M.** (1979). Allometry of the limb bones of mammals from shrew (*Sorex*) to elephant (*Loxodonta*). *J. Zool., Lond.* **189**, 305–314.

**Biewener, A. A.** (1983). Allometry of quadrupedal locomotion: the scaling of duty factor, bone curvature and limb orientation to body size. *J. Exp. Biol.* **105**, 147–171.

**Biewener, A. A.** (1989). Scaling body support in mammals: limb posture and muscle mechanics. *Science* **245**, 45–48.

**Blickhan, R.** (1989). The spring-mass model for running and hopping. *J. Biomech.* **22**, 1217–1227.

**Blickhan, R. and Full, R. J.** (1993). Similarity in multilegged locomotion: bouncing like a monopode. *J. Comp. Physiol. A* **173**, 509–517.

**Calder III, W. A.** (1996). *Size, Function and Life History*. Mineola: Dover.

**Cavagna, G. A., Franzetti, P., Heglund, N. C. and Willems, P.** (1988). The determinants of the step frequency in running, trotting and hopping in man and other vertebrates. *J. Physiol., Lond.* **399**, 81–92.

**Donelan, J. M., Kram, R. and Kuo, A. D.** (2002). Simultaneous positive and negative external mechanical work in human walking. *J. Biomech.* **35**, 117–124.

**Eyzaguirre, C. and Fidone, S. J.** (1975). *Physiology of the Nervous System* Second edition. Chicago: Yearbook Medical Publishers.

**Farley, C. T., Glasheen, J. and McMahon, T. A.** (1993). Running springs: speed and animal size. *J. Exp. Biol.* **185**, 71–86.

**Fedak, M. A., Heglund, N. C. and Taylor, C. R.** (1982). Energetics and mechanics of terrestrial locomotion. II. Kinetic energy changes of the limbs and body as a function of speed and body size in birds and mammals. *J. Exp. Biol.* **97**, 23–40.

**Full, R. J.** (1989). Mechanics and energetics of terrestrial locomotion: from bipeds to polypeds. In *Energy Transformations in Cells and Organisms* (ed. W. Wieser and E. Gnaiger), pp. 175–182. Stuttgart: Thieme.

**Full, R. J. and Koditschek, D. E.** (1999). Templates and anchors: neuromechanical hypotheses of legged locomotion on land. *J. Exp. Biol.* **202**, 3325–3332.

**Goldberg, D. E.** (1989). *Genetic Algorithms in Search, Optimization and Machine Learning*. Reading: Addison Wesley Longman.

**Gray, J.** (1968). *Animal Locomotion*. London: Weidenfeld & Nicolson.

**Heglund, N. C. and Taylor, C. R.** (1988). Speed, stride frequency and energy cost per stride: how do they change with body size and gait? *J. Exp. Biol.* **138**, 301–318.

**Heglund, N. C., Taylor, C. R. and McMahon, T. A.** (1974). Scaling stride frequency and gait to animal size: mice to horses. *Science* **186**, 1112–1113.

**Herr, H. M. and McMahon, T. A.** (2000). A trotting horse model. *Int. J. Robot. Res.* **19**, 566–581.

**Herr, H. M. and McMahon, T. A.** (2001). A galloping horse model. *Int. J. Robot. Res.* **20**, 26–41.

**Hildebrand, M.** (1976). Analysis of tetrapod gaits: general considerations and symmetrical gaits. In *Neural Control of Locomotion* (ed. R. N. Herman, S. Grillner, P. S. Stein and D. G. Stuart), pp. 203–236. New York: Plenum Press.

**Hill, A. V.** (1950). The dimensions of animals and their muscular dynamics. *Sci. Progr.* **38**, 209–230.

**Hoyt, D. F. and Taylor, C. R.** (1981). Gait and the energetics of locomotion in horses. *Nature* **292**, 239–240.

**Kram, R. and Taylor, C. R.** (1990). Energetics of running: a new perspective. *Nature* **346**, 265–267.

**Kubow, T. M. and Full, R. J.** (1999). The role of the mechanical system in control: a hypothesis of self-stabilization in hexapedal runners. *Phil. Trans. R. Soc. Lond. B* **354**, 849–861.

**Lee, D. V., Bertram, J. E. A. and Todhunter, R. J.** (1999). Acceleration and balance in trotting dogs. *J. Exp. Biol.* **202**, 3565–3573.

**Margaria, R.** (1976). *Biomechanics and Energetics of Muscular Exercise*. Oxford: Clarendon.

**McMahon, T. A.** (1973). Size and shape in biology. *Science* **179**, 1201–1204.

**McMahon, T. A.** (1975). Using body size to understand the structural design of animals: quadrupedal locomotion. *J. Appl. Physiol.* **39**, 619–627.

**McMahon, T. A.** (1977). Scaling quadrupedal galloping: frequencies, stresses and joint angles. In *Scale Effects in Animal Locomotion* (ed. T. J. Pedley), pp. 143–151. New York: Academic Press.

**McMahon, T. A. and Cheng, G. C.** (1990). The mechanics of running: how does stiffness couple with speed? *J. Biomech.* **23 (Suppl. 1)**, 65–78.

**Muybridge, E.** (1957). *Animals in Motion*. Mineola: Dover.

**Nise, N. S.** (1995). *Control Systems Engineering.* Menlo Park: Addison-Wesley.

**Raibert, M. H. and Hodgins, J. K.** (1993). Legged robots. In *Biological Neural Networks in Invertebrate Neuroethology and Robotics* (ed. R. D. Beer, R. E. Ritzmann and T. McKenna), pp. 319–354. Boston: Academic Press.

**Roberts, T. J.** (1995). Running economically: form, gait and muscle mechanics. PhD thesis, Harvard University.

**Schmidt-Nielsen, K.** (1984). *Scaling: Why is Animal Size so Important?* Cambridge: Cambridge University Press.

**Taylor, C. R., Heglund, N. C. and Maloiy, G. M. O.** (1982). Energetics and mechanics of terrestrial locomotion. I. Metabolic energy consumption as a function of speed and body size in birds and mammals. *J. Exp. Biol.* **97**, 1–21.

**Taylor, C. R., Schmidt-Nielsen, K. and Raab, J. L.** (1970). Scaling of energetic cost of running to body size in mammals. *Am. J. Physiol*. **219**, 1104–1107.

**Taylor, C. R., Shkolnik, A., Dmi'el, R., Baharav, D. and Borut, A.** (1974). Running in cheetahs, gazelles and goats: energy cost and limb configuration. *Am. J. Physiol*. **227**, 848–850.